*Journal of Advanced Research in Fluid Mechanics and Thermal Sciences* 98, Issue 1 (2022) 1-17

Journal of Advanced Research in Fluid Mechanics and Thermal Sciences

Journal homepage:
https://semarakilmu.com.my/journals/index.php/fluid_mechanics_thermal_sciences/index
ISSN: 2289-7879

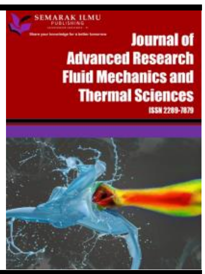


# Peristaltic Transport of Carreau Coupled Stress Nanofluid with Cattaneo-Christov Heat Flux Model Inside a Symmetric Channel

Yasmeen Mostafa Mohamed[1,*], Nabil Tafik El-Dabe[1], Mohamed Yahya Abou-Zeid[1], Mahmoud Elhassan Oauf[1], Doaa Roshhdy Mostapha[1]

[1] Department of Math., Faculty of Education, Ain Shams University, Roxy, Cairo, Egypt

**ARTICLE INFO**

***Article history:***
Received 17 March 2022
Received in revised form 13 June 2022
Accepted 25 June 2022
Available online 19 July 2022

***Keywords:***
Peristaltic flow; Cattaneo-Christov heat flux; Carreau fluid model; nanofluid; Couple stress; heat and mass transfer

**ABSTRACT**

The current analytical study is concerned with studying the impact of Cattaneo-Christov heat flux of an incompressible flow which obeys Carreau nanofluid inside a symmetric channel in the existence of the porous medium. The impacts of couple stress, heat generation absorption, joule heating, couple stress viscous dissipation with Soret as well as Dufour numbers are all presumed. Long wavelength and law Reynold's number approximations are utilized for solving the governing system of equations. Furthermore, the traditional perturbation method together with the homotopy perturbation technique (HPM) are applied to obtain the resultant solutions of these equations. The different physical parameters on velocity, temperature and nanoparticles concentration distributions are illustrated through a set of graphs. It is found that the elevate in the slip velocity parameter dwindle the velocity. Meanwhile, the rise in the value of thermal relaxation time parameter led to decay the temperature of the fluid. Over and above, enhancing the nano Biot number value caused an enrichment in the concentration of nanofluid.

## 1. Introduction

Heat transfer phenomenon results from difference of temperature between two different kinds of bodies. Among the applications of transmission of mass and heat are the formation of polyethylene and papers, conduction of heat in tissues, crystals growth, cooling of nuclear reactors, castings of metals, cooling of metallic sheet in the cooling bath, latent heat storage, and biomedical aspects including drug targeting and other applications [1-4]. Heat transfer processes were first explored by Fourier [5] whose work revealed that energy profile is parabolic in nature. Afterward, Cattaneo [6] modified Fourier's law by adding the thermal relaxation time factor so that the heat is transferred in the thermal wave form with a finite speed. Subsequently, Christov [7] developed the model of Cattaneo, which is called the Cattaneo–Christov heat flux model. Numerous research works were conducted to analyze the impacts of Cattaneo-Christov heat flux [8-19].

* *Corresponding author.*
*E-mail address: yasmeenmostafa@edu.asu.edu.eg*

https://doi.org/10.37934/arfmts.98.1.117

Nanofluids are instrumental in a wide variety of industrial and technological devices as well as engineering applications, of which the most significant are heat exchanger, fuel cells, cooling of electronic devices, development of chemical and biosensors, and hybrid power engine, etc. These fluids are mainly utilized to modulate thermal conductivity and heat transfer in such a way as to achieve the better. Given the importance of these several important applications, many researchers have paid considerable attention to the study of nanofluids [20-32].

The peristaltic transport of non-Newtonian nanofluid has been instrumental in biomedical engineering. Peristaltic flow is regarded as a method of fluid transport, which is induced by a progressive wave of area contraction or expansion along the flexible walls of a channel. Transport of blood in vessels, industrial pumping, and driving urine from the kidneys to the bladder are among the uses of these flows. Fluid trapping and material reflux are two interesting phenomena related to peristaltic flows. The peristaltic flow mechanism has become a major concern of numerous researchers [33-38].

Based on the previous literature, it is found that no study has paid attention to the influences of peristaltic nanofluid flow together with the Cattaneo-Christov heat flux model. Moreover, further terms which are associated with Brownian motion and thermophoresis impacts, and which appear under the theory of Cattaneo–Christov are missing in the previous studies. Furthermore, the influence of Cattaneo- Christov heat flux with the peristaltic nanofluid flow was not addressed in the preceding studies, excluding Eldabe *et al.,* [39] where Cattaneo-Christov double diffusion effectiveness on non-Newtonian nanofluid peristaltic influx was investigated. Thus, the essential motivation of this analytical study focusses on studying the influence of the Cattaneo-Christov heat flux model as well as couple stress on nanofluid peristaltic flow through a symmetric channel. The impacts of heat generation, the permeability of the medium, Soret and Dufour effects, viscous dissipation and chemical reaction are also imposed. Moreover, the influence of slip condition for the distributions of the axial velocity is considered. Furthermore, the convective condition for distributions of nanofluid concentration is also presumed. The mathematical intricacy of this study can be alleviating by utilizing the presumptions of long wavelength and low Reynolds number. The resultant non-linear equations are analytically disbanded by applying the conventional perturbation method together with HPM. The influences of assorted physical parameters on the various distributions are analyzed numerically and displayed through a set of graphs.

## 2. Mathematical Formulation

The nanofluid peristaltic influx in a symmetric horizontal channel of width $2a_0$ is imposed. The system of Cartesian coordinate $(\zeta_1, \xi_1)$ in the fixed frame is utilized. The $\zeta_1$ −axis is hypothesized to be in the wave prevalence orientation**,** whereas $\xi_1$ −axis is vertical to it. The channel's walls are deemed to be of resilient kind. **S**inusoidal waves of protracted wavelength $\lambda_0$ travelling with a fixed speed $c_d$ over the channel's walls generate the flow. The lower wall is kept at a temperature $T_0^e$, and nanoparticles phenomena $f_0^n$. The upper wall is kept at a temperature $T_1^e$, and nanoparticles phenomena $f_1^n$. The physical model is graphed as seen in Figure 1.

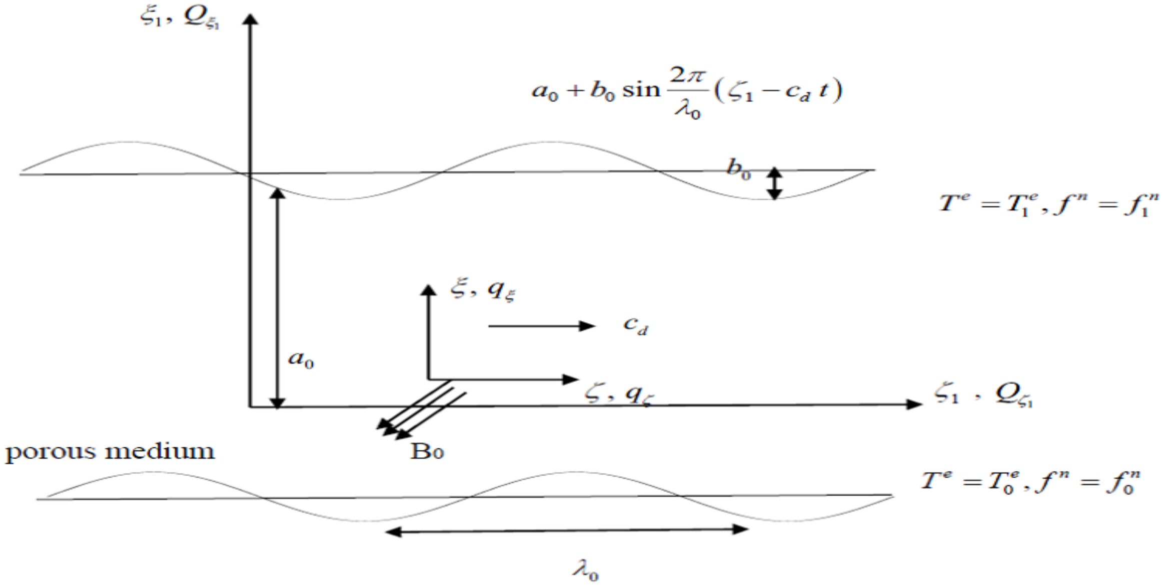


**Fig. 1.** Diagram of fluid influx

The equation of the surface written as

$$\xi_1 = \pm H_0(\zeta_1, t) = \pm\left[a_0 + b_0\, sin\frac{2\pi}{\lambda_0}(\zeta_1 - c_d t)\right] \tag{1}$$

The Carreau fluid Cauchy stress tensor $\underline{\tau^c}$ may be introduced as [35]

$$\underline{\tau^c} = -\,\mathrm{P}_e\,\mathrm{I} + \mu_s(\dot{\varsigma})\,\underline{A}_{1\mathrm{c}} \tag{2}$$

$$\mu_s(\dot{\varsigma}) = \mu_{s\infty} + (\mu_{s0} - \mu_{s\infty})\left[1 + (\Gamma_1^c\dot{\varsigma})^2\right]^{\frac{n_c-1}{2}} \tag{3}$$

$$\dot{\varsigma} = \sqrt{\frac{1}{2}\Theta_c} \tag{4}$$

$$\Theta_c = tr(\underline{A}_{1c}^2) \tag{5}$$

$$\underline{A}_{1\mathrm{c}} = (\nabla\underline{Q}) + (\nabla\underline{Q})^T \tag{6}$$

The shear thinning fluid is obtained for $(0 < n_c < 1)$, whilst it's observed that the fluid behavior is the same as the shear thickening when $(n_c > 1)$. Finally, for $n_c = 1$, or for $\Gamma_1^c = 1$ the fluid is reduced to the Newtonian case. Thus, by using different values of the Carreau fluid power index $n_c$, several various fluids can be examined. Consider the case when $\mu_{s\infty} = 0$, and $\Gamma_1^c\dot{\varsigma} \ll 1$.

Thus, the viscosity of the Carreau fluid model may be rewritten as follows

$$\mu_s(\dot{\varsigma}) = \mu_{s0}\left[1 + \left(\Gamma_1^c \dot{\varsigma}\right)^2\right]^{\frac{n_c-1}{2}} \tag{7}$$

Now, the transformations between the fixed frame $(\zeta_1, \xi_1)$and the wave frame $(\zeta, \xi)$which moves with the speed $c$ are represented as follows

$$\begin{gathered}\zeta = \zeta_1 - c_d t, \xi = \xi_1, q_\zeta(\zeta, \xi) = Q_{\zeta_1}(\zeta_1, \xi_1; t) - c_d \\ q_\xi(\zeta, \xi) = Q_{\xi_1}(\zeta_1, \xi_1; t), T^e(\zeta, \xi) = T^e(\zeta_1, \xi_1; t) \\ f^n(\zeta, \xi) = f^n(\zeta_1, \xi_1; t)\end{gathered} \tag{8}$$

where, $\left(Q_{\zeta_1}, Q_{\xi_1}\right)$ are the ingredients of the velocity components in stationary frame. Whereas $\left(q_\zeta, q_\xi\right)$ are in the moving frame. The conducting fluid is permeated by an imposed magnetic field $B_0$, which acts in $z-$ axis direction i.e., $\underline{B} = (0,0, B_0)$. For low-Reynolds magnetic field, the induced magnetic field and external electric field are neglected.

Following [33,34,39], the polarization voltage isn't taken into our consideration (*i.e.,* the total electric field is vanishing $\underline{E_l} = \underline{0}$). Thus, the current density $\underline{J_1}$ may be expressed as follows

$$\underline{J_1} = \sigma_c\left(\underline{Q} \wedge \underline{B}\right) \tag{9}$$

Energy equation can be expressed as

$$\begin{aligned}(\rho c)_s \frac{dT^e}{dt} = -\nabla \cdot \underline{q_H} + (\rho c)_n\left[D_N(\nabla T^e \cdot \nabla f^n) + \frac{D_H}{T_0^e}(\nabla T^e \cdot \nabla T^e)\right] + \left(\underline{\tau}_{Couple} \cdot \nabla \underline{Q}\right)_{Couple} \\ + R_G(T^e - T_0^e) + \frac{D_N K_H}{C_{en}} \nabla^2 f^n\end{aligned} \tag{10}$$

*2.1 Cattaneo – Christov Heat Influx Model*

Cattaneo – Christov heat inflow model may be defined as [8, 10, 11, 39]

$$\begin{aligned}\underline{q_H} + \lambda_H\left[\frac{\partial \underline{q_H}}{\partial t} + \underline{Q} \cdot \nabla \underline{q_H} - \underline{q_H} \cdot \nabla \underline{Q} + \left(\nabla \cdot \underline{Q}\right) \underline{q_H}\right] \\ = -K_1^e \nabla T^e\end{aligned} \tag{11}$$

which is the generalized Fourier's law. In case $(\lambda_H = 0)$, the classical Fourier's heat flux law of diffusion is retained. For the incompressible fluid, we have $\left(\nabla \cdot \underline{Q} = 0\right)$. Thus, Eq. (11) can be rewritten as follows

$$\underline{q_H} + \lambda_H\left[\frac{\partial \underline{q_H}}{\partial t} + \underline{Q} \cdot \nabla \underline{q_H} - \underline{q_H} \cdot \nabla \underline{Q}\right] = -K_1^e \nabla T^e \tag{12}$$

## 3. The Equations that Govern the Fluid Motion

After applying Eq. (8), these equations may be expressed as follows

$$\frac{\partial q_\zeta}{\partial \zeta}+\frac{\partial q_\xi}{\partial \xi}=0 \tag{13}$$

$$\rho_s\left(q_\zeta \frac{\partial q_\zeta}{\partial \zeta}+q_\xi \frac{\partial q_\zeta}{\partial \xi}\right) =-\frac{\partial P_e}{\partial \zeta}+\frac{\partial \tau_{\zeta\zeta}^c}{\partial \zeta}+\frac{\partial \tau_{\zeta\xi}^c}{\partial \xi}-\left(\sigma_c B_0^2+\frac{\mu_{s0}}{K_1^p}\right)q_\zeta-\eta_1^c\left(\frac{\partial^4 q_\zeta}{\partial \zeta^4}+2\frac{\partial^4 q_\zeta}{\partial \zeta^2\partial \xi^2}+\frac{\partial^4 q_\zeta}{\partial \xi^4}\right) \tag{14}$$

$$\rho_s\left(q_\zeta \frac{\partial q_\xi}{\partial \zeta}+q_\xi \frac{\partial q_\xi}{\partial \xi}\right) =-\frac{\partial P_e}{\partial \xi}+\frac{\partial \tau_{\xi\zeta}^c}{\partial \zeta}+\frac{\partial \tau_{\xi\xi}^c}{\partial \xi}-\left(\sigma_c B_0^2+\frac{\mu_{s0}}{K_1^p}\right)q_\xi-\eta_1^c\left(\frac{\partial^4 q_\xi}{\partial \zeta^4}+2\frac{\partial^4 q_\xi}{\partial \zeta^2\partial \xi^2}+\frac{\partial^4 q_\xi}{\partial \xi^4}\right) \tag{15}$$

$$\begin{aligned}(\rho c)_s\left(q_\zeta \frac{\partial T^e}{\partial \zeta}+\mathrm{q}_\xi \frac{\partial T^e}{\partial \xi}\right)+\lambda_H \Xi_H &= K_1^e\left(\frac{\partial^2 T^e}{\partial \zeta^2}+\frac{\partial^2 T^e}{\partial \xi^2}\right)+\frac{D_N K_H}{C_{en}}\left(\frac{\partial^2 f^n}{\partial \zeta^2}+\frac{\partial^2 f^n}{\partial \xi^2}\right)\\ &+(\rho c)_n\left[D_N\left(\frac{\partial T^e}{\partial \zeta}\frac{\partial f^n}{\partial \zeta}+\frac{\partial T^e}{\partial \xi}\frac{\partial f^n}{\partial \xi}\right)+\frac{D_H}{T_0^e}\left(\left(\frac{\partial T^e}{\partial \zeta}\right)^2+\left(\frac{\partial T^e}{\partial \xi}\right)^2\right)\right]+R_G(T^e-T_0^e)\\ &-\eta_1^c\left(\begin{aligned}&2\frac{\partial q_\zeta}{\partial \zeta}\frac{\partial^3 q_\zeta}{\partial \zeta^3}+2\frac{\partial q_\zeta}{\partial \zeta}\frac{\partial^3 q_\zeta}{\partial \xi^2\partial \zeta}+2\frac{\partial q_\xi}{\partial \xi}\frac{\partial^3 q_\xi}{\partial \xi\partial \zeta^2}+2\frac{\partial q_\xi}{\partial \xi}\frac{\partial^3 q_\xi}{\partial \xi^3}\\ &+\frac{\partial q_\zeta}{\partial \xi}\frac{\partial^3 q_\zeta}{\partial \xi^3}+\frac{\partial q_\zeta}{\partial \xi}\frac{\partial^3 q_\xi}{\partial \zeta^3}+\frac{\partial q_\xi}{\partial \zeta}\frac{\partial^3 q_\zeta}{\partial y^3}+\frac{\partial q_\xi}{\partial \zeta}\frac{\partial^3 q_\xi}{\partial \zeta^3}\end{aligned}\right)\\ &+\sigma_c B_0^2\left(q_\zeta^2+q_\xi^2\right)\end{aligned} \tag{16}$$

$$q_\zeta \frac{\partial f^n}{\partial \zeta}+\mathrm{q}_\xi \frac{\partial f^n}{\partial \xi}=D_N\left(\frac{\partial^2 f^n}{\partial \zeta^2}+\frac{\partial^2 f^n}{\partial \xi^2}\right)+\left(\frac{D_H}{T_0^e}+\frac{D_N K_H}{T_m^e}\right)\left[\frac{\partial^2 T^e}{\partial \zeta^2}+\frac{\partial^2 T^e}{\partial \xi^2}\right]-K_0^n(f^n-f_0^n) \tag{17}$$

where,

$$\begin{aligned}\varXi_H = (\rho c)_s &\left[q_\zeta^2 \frac{\partial^2 T^e}{\partial \zeta^2} + 2q_\zeta q_\xi \frac{\partial^2 T^e}{\partial \zeta \partial \xi} + q_\xi^2 \frac{\partial^2 T^e}{\partial \xi^2} + \left(q_\zeta \frac{\partial q_\zeta}{\partial \zeta} + q_\xi \frac{\partial q_\zeta}{\partial \xi}\right)\frac{\partial T^e}{\partial \xi}\right.\\
&\left. + \left(q_\zeta \frac{\partial q_\xi}{\partial \zeta} + q_\xi \frac{\partial q_\xi}{\partial \xi}\right)\frac{\partial T^e}{\partial \xi}\right] - \frac{D_N K_H}{C_{en}}\left(q_\zeta\left(\frac{\partial^3 f^n}{\partial \zeta^3} + \frac{\partial^3 f^n}{\partial \zeta \partial \xi^2}\right) + q_\xi\left(\frac{\partial^3 f^n}{\partial \xi^3} + \frac{\partial^3 f^n}{\partial \xi \partial \zeta^2}\right)\right)\\
&- 2\sigma_c B_0^2\left(q_\zeta^2 \frac{\partial u}{\partial \zeta} + q_\zeta q_\xi\left(\frac{\partial u}{\partial \xi} + \frac{\partial v}{\partial \zeta}\right) + q_\xi^2 \frac{\partial v}{\partial \xi}\right)\\
&- (\rho c)_n \left[\begin{matrix} D_N\left(\left(\frac{\partial T^e}{\partial \xi}\left(q_\zeta \frac{\partial^2 f^n}{\partial \zeta \partial \xi} + q_\xi \frac{\partial^2 f^n}{\partial \xi^2}\right) + \frac{\partial f^n}{\partial \xi}\left(q_\zeta \frac{\partial^2 T^e}{\partial \zeta \partial \xi} + q_\xi \frac{\partial^2 T^e}{\partial \xi^2}\right)\right)\right) \\ +2\frac{D_H}{T_0^e}\left(\frac{\partial T^e}{\partial \zeta}\left(q_\zeta \frac{\partial^2 T^e}{\partial \zeta^2} + q_\xi \frac{\partial^2 T^e}{\partial \zeta \partial \xi}\right) + \frac{\partial T^e}{\partial \xi}\left(q_\zeta \frac{\partial^2 T^e}{\partial \zeta \partial \xi} + q_\xi \frac{\partial^2 T^e}{\partial \xi^2}\right)\right)\end{matrix}\right]\\
&- R_G\left(q_\zeta \frac{\partial T^e}{\partial \zeta} + q_\xi \frac{\partial T^e}{\partial \xi}\right) -
\end{aligned}$$

$$\eta_1^c \begin{pmatrix} 2q_\zeta \frac{\partial^2 q_\zeta}{\partial \zeta^2}\frac{\partial^3 q_\zeta}{\partial \zeta^3} + 2q_\xi \frac{\partial^2 q_\zeta}{\partial \zeta \partial \xi}\frac{\partial^3 q_\zeta}{\partial \zeta^3} + 2q_\zeta \frac{\partial q_\zeta}{\partial \zeta}\frac{\partial^4 q_\zeta}{\partial \zeta^4} + 2q_\xi \frac{\partial q_\zeta}{\partial \zeta}\frac{\partial^4 q_\zeta}{\partial \xi \partial \zeta^3} + 2q_\zeta \frac{\partial^2 q_\zeta}{\partial \zeta^2}\frac{\partial^3 q_\zeta}{\partial \zeta \partial \xi^2} \\
+2q_\zeta \frac{\partial q_\zeta}{\partial \zeta}\frac{\partial^4 q_\zeta}{\partial \xi^2 \partial \zeta^2} + 2q_\xi \frac{\partial^2 q_\zeta}{\partial \zeta \partial \xi}\frac{\partial^3 q_\zeta}{\partial \zeta \partial \xi^2} + 2q_\xi \frac{\partial q_\zeta}{\partial \zeta}\frac{\partial^4 q_\zeta}{\partial \zeta \partial \xi^3} + 2q_\zeta \frac{\partial^2 q_\xi}{\partial \zeta \partial \xi}\frac{\partial^3 q_\xi}{\partial \xi \partial \zeta^2} + 2q_\zeta \frac{\partial q_\xi}{\partial \xi}\frac{\partial^4 q_\xi}{\partial \xi \partial \zeta^3} \\
+2q_\xi \frac{\partial^2 q_\xi}{\partial \xi^2}\frac{\partial^3 q_\xi}{\partial \xi \partial \zeta^2} + 2q_\xi \frac{\partial q_\xi}{\partial \xi}\frac{\partial^4 q_\xi}{\partial \xi^2 \partial \zeta^2} + 2q_\zeta \frac{\partial^2 q_\xi}{\partial \zeta \partial \xi}\frac{\partial^3 q_\xi}{\partial \xi^3} + 2q_\zeta \frac{\partial q_\xi}{\partial \xi}\frac{\partial^4 q_\xi}{\partial \zeta \partial \xi^3} + 2q_\xi \frac{\partial^2 q_\xi}{\partial \xi^2}\frac{\partial^3 q_\xi}{\partial \xi^3} \\
+2q_\xi \frac{\partial q_\xi}{\partial \xi}\frac{\partial^4 q_\xi}{\partial \xi^4} + q_\zeta \frac{\partial^2 q_\zeta}{\partial \zeta \partial \xi}\frac{\partial^3 q_\zeta}{\partial \xi^3} + q_\zeta \frac{\partial q_\zeta}{\partial \xi}\frac{\partial^4 q_\zeta}{\partial \zeta \partial \xi^3} + q_\xi \frac{\partial^2 q_\zeta}{\partial \xi^2}\frac{\partial^3 q_\zeta}{\partial \xi^3} + q_\xi \frac{\partial q_\zeta}{\partial \xi}\frac{\partial^4 q_\zeta}{\partial \xi^4} + q_\zeta \frac{\partial q_\zeta}{\partial \xi}\frac{\partial^4 q_\xi}{\partial \zeta^4} \\
+q_\xi \frac{\partial^2 q_\zeta}{\partial \xi^2}\frac{\partial^3 v}{\partial \zeta^3} + q_\xi \frac{\partial q_\zeta}{\partial \xi}\frac{\partial^4 q_\xi}{\partial \zeta^3 \partial \xi} + q_\zeta \frac{\partial^3 q_\zeta}{\partial \xi^3}\frac{\partial^2 q_\xi}{\partial \zeta^2} + q_\zeta \frac{\partial q_\xi}{\partial \zeta}\frac{\partial^4 q_\zeta}{\partial \zeta \partial \xi^3} + q_\xi \frac{\partial^2 q_\xi}{\partial \zeta \partial \xi}\frac{\partial^3 q_\zeta}{\partial \xi^3} + q_\xi \frac{\partial q_\xi}{\partial \zeta}\frac{\partial^4 q_\zeta}{\partial \xi^4} \\
+q_\zeta \frac{\partial^2 q_\xi}{\partial \zeta^2}\frac{\partial^3 q_\xi}{\partial \zeta^3} + q_\zeta \frac{\partial q_\xi}{\partial \zeta}\frac{\partial^4 q_\xi}{\partial \zeta^4} + q_\xi \frac{\partial^2 q_\xi}{\partial \zeta \partial \xi}\frac{\partial^3 q_\xi}{\partial \zeta^3} + q_\xi \frac{\partial q_\xi}{\partial \zeta}\frac{\partial^4 q_\xi}{\partial \zeta^3 \partial \xi}
\end{pmatrix} \tag{18}$$

The stream function $\psi(x, y)$ can be introduced as follows:

$$q_\zeta = \frac{\partial \Psi_s}{\partial \xi}\ and\ \ q_\xi = -\frac{\partial \Psi_s}{\partial \zeta} \tag{19}$$

The dimensionless variables are introduced as:

$$W_e^c = \frac{\Gamma_1^c c_d}{a_0}, \zeta^* = \frac{\zeta}{\lambda_0}, \xi^* = \frac{\xi}{a_0}, \delta_1 = \frac{a_0}{\lambda_0}, \varepsilon_0 = \frac{b_0}{a_0}, \psi_s^* = \frac{\Psi_s}{c_d a_0}, \Gamma_H = \frac{c_d \lambda_H}{a_0}, R_{en} = \frac{\rho_s c_d a_0}{\mu_{s0}}, P_m^* = \frac{P_e a_0^2}{\lambda_0 c_d \mu_{s0}}, 60°$$

$$H_0^* = \frac{H_0}{a_0}, v_s = \frac{\mu_{s0}}{\rho_s}, \theta_E = \frac{T^e - T_0^e}{T_1^e - T_0^e}, F_N = \frac{f^n - f_0^n}{f_1^n - f_0^n}, B_{m1} = \frac{L_{n1} a_0}{D_N}, B_{m2} = \frac{L_{n2} a_0}{D_N}, P_{ra} = \frac{c_s \mu_{s0}}{K_1^e}$$

$$B_{rk} = E_{ck} P_{ra}, \gamma_c^2 = \frac{\mu_{s0} a_0^2}{\eta_1^c}, S_{or} = \frac{D_N K_H (T_1^e - T_0^e)}{v_s T_m^e (f_1^n - f_0^n)}, M_F^2 = \frac{\sigma_c B_0^2 a_0^2}{\mu_{s0}}, D_{Ar} = \frac{K_1^p}{a_0^2}, R_{cr} = \frac{K_0^n a_0^2}{v_f} \tag{20}$$

$$S_{ch} = \frac{v_s}{D_N}, \tau_s^n = \frac{(\rho c)_n}{(\rho c)_s}, N_{th} = \frac{\tau_s^n D_T (T_1^e - T_0^e)}{v_s T_0^e}, D_f = \frac{D_N K_H (f_1^n - f_0^n)}{c_n v_s C_{en} (T_1^e - T_0^e)}, N_{br} = \frac{\tau_s^n D_N (f_1^n - f_0^n)}{v_s}$$

$$\beta_1^s=\frac{\beta^*}{a_0},\beta_H=\frac{R_G a_0^2}{K_1^e c_s},E_{ck}=\frac{c_d^2}{c_s(T_1^e-T_0^e)},\tau_{\xi\xi}^{c*}=\frac{a_0}{c_d\mu_{s0}}\tau_{\xi\xi},\tau_{\zeta\xi}^{c*}=\frac{a_0}{c_d\mu_{s0}}\tau_{\zeta\xi},\tau_{\zeta\zeta}^{c*}=\frac{a_0}{c_d\mu_{s0}}\tau_{\zeta\zeta}$$

By differentiating Eq. (14) w.r.to y and Eq. (15) w.r.to x then subtract the results to eliminate the pressure. After that utilize the approximations of the long wavelength $(\delta_1 << 1)$with low Reynolds number $(R_{en} \ll 1)$, and substituting from Eq. (19) and (20) into Eq. (13)-(18). Thereafter, for facilitating star marks are disregarded. Thus, the dimensionless differential equations become

$$\begin{aligned}&R_{en}\delta_1\left(\psi_{s\xi}\frac{\partial^3\psi_s}{\partial\zeta\partial\xi^2}-\psi_{s\zeta}\frac{\partial^3\psi_s}{\partial\xi^3}\right)\\&=-\frac{1}{\gamma_c^2}\frac{\partial^6\psi_s}{\partial\xi^6}+\frac{\partial^4\psi_s}{\partial\xi^4}-\left(M_F^2+\frac{1}{D_{Ar}}\right)\frac{\partial^2\psi_s}{\partial\xi^2}+\frac{3(n_c-1)}{2}W_e^{c2}\left(\frac{\partial^2\psi_s}{\partial\xi^2}\right)^2\frac{\partial^4\psi_s}{\partial\xi^4}\\&+\frac{6(n_c-1)}{2}W_e^{c2}\left(\frac{\partial^3\psi_s}{\partial\xi^3}\right)^2\frac{\partial^2\psi_s}{\partial\xi^2}\end{aligned}\tag{21}$$

$$\begin{aligned}&\frac{\partial^2\theta_E}{\partial\xi^2}\\&=R_{en}P_{ra}\delta_1\left(\psi_{s\xi}\frac{\partial\theta_E}{\partial\zeta}-\psi_{s\zeta}\frac{\partial\theta_E}{\partial\xi}\right)-P_{ra}N_{br}\left(\frac{\partial\theta_E}{\partial\xi}\right)\left(\frac{\partial F_N}{\partial\xi}\right)-P_{ra}N_{th}\left(\frac{\partial\theta_E}{\partial\xi}\right)^2-P_{ra}\beta_H\theta_E\\&-\frac{B_{rk}}{\gamma_c^2}\frac{\partial^2\psi_s}{\partial\xi^2}\frac{\partial^4\psi_s}{\partial\xi^4}-M_F^2B_{rk}\left(\frac{\partial\psi_s}{\partial\xi}\right)^2-D_fB_{rk}\frac{\partial^2F_N}{\partial\xi^2}\\&-\delta_1\Gamma_H\left[\begin{array}{l}P_{ra}N_{br}\left(\psi_{s\xi}\left(\frac{\partial F_N}{\partial\xi}\frac{\partial^2\theta_E}{\partial\zeta\partial\xi}+\frac{\partial\theta_E}{\partial\xi}\frac{\partial^2F_N}{\partial\zeta\partial\xi}\right)-\psi_{s\zeta}\left(\frac{\partial F_N}{\partial\xi}\frac{\partial^2\theta_E}{\partial\xi^2}+\frac{\partial\theta_E}{\partial\xi}\frac{\partial^2F_N}{\partial\xi^2}\right)\right)+\\2P_{ra}N_{th}\left(\psi_{s\xi}\frac{\partial\theta_E}{\partial\xi}\frac{\partial^2\theta_E}{\partial\zeta\partial\xi}-\psi_{s\zeta}\frac{\partial\theta_E}{\partial\xi}\frac{\partial^2\theta_E}{\partial\xi^2}\right)+P_{ra}\beta_H\left(\psi_{s\xi}\frac{\partial\theta_E}{\partial\zeta}-\psi_{s\zeta}\frac{\partial\theta_E}{\partial\xi}\right)+\\2M_F^2B_{rk}\left(\left(\frac{\partial\psi_s}{\partial\xi}\right)^2\frac{\partial^2\psi_s}{\partial\zeta\partial\xi}-\psi_{s\zeta}\psi_{s\xi}\frac{\partial^2\psi_s}{\partial\xi^2}\right)+D_fB_{rk}\left(\psi_{s\xi}\frac{\partial^3F_N}{\partial\zeta\partial\xi^2}-\psi_{s\zeta}\frac{\partial^3F_N}{\partial\xi^3}\right)\\+\frac{B_{rk}}{\gamma_c^2}\left(\psi_{s\xi}\left(\frac{\partial^4\psi_s}{\partial\xi^4}\frac{\partial^3\psi_s}{\partial\zeta\partial\xi^2}+\frac{\partial^2\psi_s}{\partial\xi^2}\frac{\partial^5\psi_s}{\partial\zeta\partial\xi^4}\right)-\psi_{s\zeta}\left(\frac{\partial^3\psi_s}{\partial\xi^3}\frac{\partial^4\psi_s}{\partial\xi^4}+\frac{\partial^2\psi_s}{\partial\xi^2}\frac{\partial^5\psi_s}{\partial\xi^5}\right)\right)\end{array}\right]\end{aligned}\tag{22}$$

$$\frac{\partial^2F_N}{\partial\xi^2}=R_{en}S_{ch}\delta_1\left(\psi_{s\xi}\frac{\partial F_N}{\partial\zeta}-\psi_{s\zeta}\frac{\partial F_N}{\partial\xi}\right)-\left(S_{or}S_{ch}+\frac{N_{th}}{N_{br}}\right)\frac{\partial^2\theta_E}{\partial\xi^2}+R_{cr}S_{ch}F_N\tag{23}$$

The convenient boundary conditions may be expressed as [33,35,39]

$$\begin{aligned}&\psi_{s\xi}=-1-\beta_1^s\left(\psi_{s\xi\xi}+\left(\frac{n_c-1}{2}\right)W_e^{c2}\left(\psi_{s\xi\xi}\right)^3\right),\psi_{s\xi\xi\xi}=0,\theta_E=0,\frac{\partial F_N}{\partial y}-B_{m1}F_N=0\\&at\ \xi=-1-\varepsilon_0\sin 2\pi\zeta\end{aligned}\tag{24}$$

$$\psi_s=0\ \text{at}\ \xi=0\tag{25}$$

$$\psi_{s\xi} = -1 - \beta_1^s\left(\psi_{s\xi\xi} + \left(\frac{n_c-1}{2}\right)W_e^{c2}\left(\psi_{s\xi\xi}\right)^3\right), \psi_{s\xi} = -1, \psi_{s\xi\xi\xi} = 0, \theta_E = 1, \frac{\partial F_N}{\partial \xi} + B_{m2}(F_N - 1) = 0$$

at $\xi = 1 + \varepsilon_0 \, sin\, 2\,\pi\zeta$ (26)

## 4. Methodology of Solution

### *4.1 Regular Perturbation Technique*

In accordance with the mechanism of conventional perturbation, the outcomes are expanded in terms of the wave number $\delta$ as

$$\varDelta = \Delta_0 + \delta_1\varDelta_1 + \delta_1^2\,\varDelta_2 + \cdots\cdots\cdots \tag{27}$$

where, $\varDelta$ points out to any one of these distributions $q_\zeta$, $\theta_E$ $F_N$

### *4.2 Homotopy Perturbation Method (HPM)*

HPM can be applied to make another approximate solution for these equations after utilizing (27). According to HPM [33,34,39-44], we suppose that $q_{\zeta 0}$, $\theta_{E0}$ and $F_{\mathrm{N}0}$ have the solution of the form

$$\varSigma_0 = \Sigma_{00} + P_H\,\varSigma_{01} + \mathrm{P}_H^2\,\varSigma_{02} + \cdots\cdots\cdots \tag{28}$$

where, $\varSigma$ refers to any one of these distributions $q_{\zeta 0}$, $\theta_{E0}$ with$F_{\mathrm{N}0}$.

The linear operators may be represented as

$$L_1\left(q_\zeta\right) = \frac{\partial^6 q_\zeta}{\partial \xi^6} \tag{29}$$

$$L_2(\theta_E) = \frac{\partial^2 \theta_E}{\partial \xi^2} \tag{30}$$

$$L_3(F_N) = \frac{\partial^2 F_N}{\partial \xi^2} - \left(S_r S_c + \frac{N_t}{N_b}\right) \tag{31}$$

The initial guessing may be presupposed as

$$q_{\zeta 00} = \frac{1}{120}\,\omega_1\xi^5 + \frac{1}{24}\,\omega_2\xi^4 + \frac{1}{6}\,\omega_3\xi^3 + \frac{1}{2}\,\omega_4\xi^2 + \omega_5\xi^2 + \omega_6 \tag{32}$$

$$\theta_{E00} = \omega_7\xi + \omega_8 \tag{33}$$

$$F_{N00} = \frac{1}{2}\left(\frac{N_{th}}{N_{br}} + S_{or}S_{ch}\right)\xi^2 + \omega_9\xi + \omega_{10} \tag{34}$$

Also, the distributions of $q_{\zeta 1}$, $\theta_{E1}$ and $F_{\mathrm{N}1}$ .have the solution of the form

$$\chi_1 = \chi_{10} + \mathrm{P}_H\, \chi_{11} + \mathrm{P}_H^2\, \chi_{12} + \cdots\cdots\cdots \tag{35}$$

where, $\chi$ stands for any one of $q_{\zeta 1}$, $\theta_{E1}$ and $F_{\mathrm{N}1}$ .

By applying the same forgoing steps and utilizing HPM as well as the linear operators definitions, the initial guesses solutions for: $q_{\zeta 1}$, $\theta_{E1}$ and $F_{\mathrm{N}1}$ may be represented as follows

$$q_{\zeta 10} = \frac{1}{120}\,\omega_{21}\xi^5 + \frac{1}{24}\,\omega_{22}\xi^4 + \frac{1}{6}\,\omega_{23}\xi^3 + \frac{1}{2}\,\omega_{24}\xi^2 + \omega_{25}\xi^2 + \omega_{26} \tag{36}$$

$$\theta_{E10} = \omega_{27}\xi + \omega_{28} \tag{37}$$

$$F_{N10} = \omega_{29}\xi + \omega_{30} \tag{38}$$

On utilizing the preceding power series solution into Eq. (21)-(26), then the complete solutions may be expressed as

$$q_\zeta = \begin{pmatrix} (\omega_6+\omega_{16}) + (\omega_5+\omega_{15})\xi + \frac{1}{2}\,(\omega_4+\omega_{14})\xi^2 + \frac{1}{6}\,(\omega_3+\omega_{13})\xi^3 \\ + \frac{1}{24}\,(\omega_2+\omega_{12})\xi^4 + \frac{1}{120}\,(\omega_1+\omega_{11})\xi^5 + \Omega_1\xi^6 + \Omega_2\xi^7 + \Omega_3\xi^8 + \Omega_4\xi^9 \\ +\Omega_5\xi^{10} + \Omega_6\xi^{11} + \Omega_7\xi^{12} + \Omega_8\xi^{13} \end{pmatrix} + \delta_1 \begin{pmatrix} (\omega_{26}+\omega_{36}) + (\omega_{25}+\omega_{35})\xi + \frac{1}{2}\,(\omega_{24}+\omega_{34})\xi^2 + \frac{1}{6}\,(\omega_{23}+\omega_{33})\xi^3 \\ + \frac{1}{24}\,(\omega_{22}+\omega_{32})\xi^4 + \frac{1}{120}\,(\omega_{21}+\omega_{31})\xi^5 + \Omega_9\xi^6 + \Omega_{10}\xi^7 + \Omega_{11}\xi^8 + \\ \Omega_{12}\xi^9 + \Omega_{13}\xi^{10} + \Omega_{14}\xi^{11} + \Omega_{15}\xi^{12} + \Omega_{16}\xi^{13} + \Omega_{17}\xi^{14} + \Omega_{18}\xi^{15} + \Omega_{19}\xi^{16} + \\ \Omega_{20}\xi^{17} + \Omega_{21}\xi^{18} + \Omega_{22}\xi^{19} + \Omega_{23}\xi^{20} + \Omega_{24}\xi^{21} + \Omega_{25}\xi^{22} + \Omega_{26}\xi^{23} + \Omega_{27}\xi^{24} \\ +\Omega_{28}\xi^{25} + \Omega_{29}\xi^{26} + \Omega_{30}\xi^{27} + \Omega_{31}\xi^{28} + \Omega_{32}\xi^{29} \end{pmatrix} \tag{39}$$

$$\theta_E = \begin{pmatrix} (\omega_8+\omega_{18}) + (\omega_7+\omega_{17})\xi + \Omega_{33}\xi^2 + \Omega_{34}\xi^3 + \Omega_{35}\xi^4 + \Omega_{36}\xi^5 + \Omega_{37}\xi^6 + \Omega_{38}\xi^7 + \\ \Omega_{39}\xi^8 + \Omega_{40}\xi^9 + \Omega_{41}\xi^{10} \end{pmatrix} + \delta_1 \begin{pmatrix} (\omega_{28}+\omega_{38}) + (\omega_{27}+\omega_{37})\xi + \Omega_{42}\xi^2 + \Omega_{43}\xi^3 + \Omega_{44}\xi^4 + \Omega_{45}\xi^5 + \Omega_{46}\xi^6 + \Omega_{47}\xi^7 + \\ \Omega_{48}\xi^8 + \Omega_{49}\xi^9 + \Omega_{50}\xi^{10} + \Omega_{51}\xi^{11} + \Omega_{52}\xi^{12} + \Omega_{53}\xi^{13} + \Omega_{54}\xi^{14} + \Omega_{55}\xi^{15} + \Omega_{56}\xi^{16} + \Omega_{57}\xi^{17} \\ + \Omega_{58}\xi^{18} + \Omega_{59}\xi^{19} + \Omega_{60}\xi^{20} + \Omega_{61}\xi^{21} + \Omega_{62}\xi^{22} + \Omega_{63}\xi^{23} + \Omega_{64}\xi^{24} + \Omega_{65}\xi^{25} + \Omega_{66}\xi^{26} \\ + \Omega_{67}\xi^{27} + \Omega_{68}\xi^{28} + \Omega_{69}\xi^{29} + \Omega_{70}\xi^{30} + \Omega_{71}\xi^{31} + \Omega_{72}\xi^{32} + \Omega_{73}\xi^{33} + \Omega_{74}\xi^{34} + \Omega_{75}\xi^{35} + \\ \Omega_{76}\xi^{36} + \Omega_{77}\xi^{37} + \Omega_{78}\xi^{38} \end{pmatrix}, \tag{40}$$

$$\mathrm{F_N} = \begin{pmatrix} (\omega_{10}+\omega_{20}) + (\omega_9+\omega_{19})\xi + \\ \left(\frac{1}{2}\left(\frac{\mathrm{N_t}}{\mathrm{N_b}} + \mathrm{S_r S_c}\right) + \Omega_{79}\right)\xi^2 + \Omega_{80}\xi^3 + \Omega_{81}\xi^4 \end{pmatrix} + \delta_1 \begin{pmatrix} (\omega_{30}+\omega_{39}) + (\omega_{29}+\omega_{40})\xi + \Omega_{82}\xi^2 + \Omega_{83}\xi^3 + \Omega_{84}\xi^4 \\ +\Omega_{85}\xi^5 + \Omega_{86}\xi^6 + \Omega_{87}\xi^7 + \Omega_{88}\xi^8 + \Omega_{89}\xi^9 + \Omega_{90}\xi^{10} + \Omega_{91}\xi^{11} \\ +\Omega_{92}\xi^{12} + \Omega_{93}\xi^{13} + \Omega_{94}\xi^{14} + \Omega_{95}\xi^{15} + \Omega_{96}\xi^{16} + \Omega_{97}\xi^{17} + \Omega_{98}\xi^{18} \end{pmatrix} \tag{41}$$

## 5. Numerical Discussions

The Mathematica software is utilized for illustrating the quantitative impacts of the diverse physical parameters on the distributions of $q_\zeta$, $\theta_E$ and $F_N$. The ranges of the dimensionless variables are imposed as [33] and [39]. ($P_{ra}=1,\ \varepsilon_0=0.2, M_F=1, \zeta=0.2,\ N_{br}=0.1,\ S_{ch}=0.5,\ S_{or}=0.5,$ $\delta_1=0.1,\ \gamma_c=2.0,\ n_c=1.5,\ \beta_H=0.5,\ \Gamma_H=1.5, D_f=0.5, \beta_1^s=0.5, R_{cr}=0.5$ and $N_{th}=0.1$).

The effect of the Weissenberg number $W_e^c$ on the axial velocity $q_\zeta$ is illustrated through Figure 2. It is found that $q_\zeta$ enhances in accordance to enrich in $W_e^c$. From the physical attitude, the Weissenberg number is inversely proportional to viscosity. Therefore, rising in $W_e^c$ deemed as reason for decaying in the viscosity of the fluid, which enlarges the axial velocity $q_\zeta$correspondingly. This demeanor is totally consistent to the behavior that reported in [15], [32], and [35]. Figure 3 portrays the impact of the velocity slip parameter$\beta_1^s$ on the axial velocity $q_\zeta$. It is recognized that when the value of $\beta_1^s$ is enhanced, the axial velocity $q_\zeta$is dwindled. Also, in case of no slip condition ($\beta_1^s = 0$)**,** the $q_\zeta$is larger than that in case of the slip parameter. In fact, the slip boundary condition or velocity offset boundary condition represents the relative movement between the fluid and the boundary. A slip parameter describes the discontinuity in the velocity function. Therefore, the elevate in $\beta_1^s$ leads to decline the axial velocity profile. This noticeable demeanor is greatly congruous to that obtained in [46].

The influences of the parameters $\gamma_c$, $M_F$and $D_{Ar}$ on $q_\zeta$ are also studied. It is noticed that all these parameters behave in the same way as the slip parameter $\beta_1^s$. The impact of the couple stress parameter $\gamma_c$ on velocity $q_\zeta$ is taken into account. It is found that the velocity profile is the decaying function under the influence of the couple stress parameter$\gamma_c$. Physically, this behavior occurs since elevating in the couple stress parameter leads to enhance the viscosity, which declines the fluid velocity. This important observation is consistent with the behavior recorded by [30], [33] and [45]. Also, velocity dwindles with an enhancement in $M_F$. As known, $M_F$ is deemed as the proportion amidst the magnetic strength and the viscid one. So, it is found that the enhancing in $M_F$ leads to reduce $q_\zeta$. From the physical visualization, this phenomenon accords with the theory which states that the rise in $M_F$increases the Lorentz force. Once noticing that the Lorentz force impedes the movement of the fluid influx. $M_F$impact has a significant role in a huge number of industrial applications, particularly in favor of solidification processes such as casting and semiconductor single crystal growth applications. In these claims, as the liquids experience solidification, fluid flow and turbulence occur in the solidifying liquid pool and have critical impacts on the product quality control. The practice of magnetic fields has effectively been applied to monitoring melt convection in solidification systems [9,10,33,35,39,47]. On the other hand, velocity is observed as an increasing function with a rise in the value of Darcy number $D_{Ar}$. From a physical perspective, the elevate in the value of Darcy number diminishes the drag force and hence enhances the flow velocity. This evident result is in a good agreement with that pointed out by [30]. These figures are excluded here to keep space.

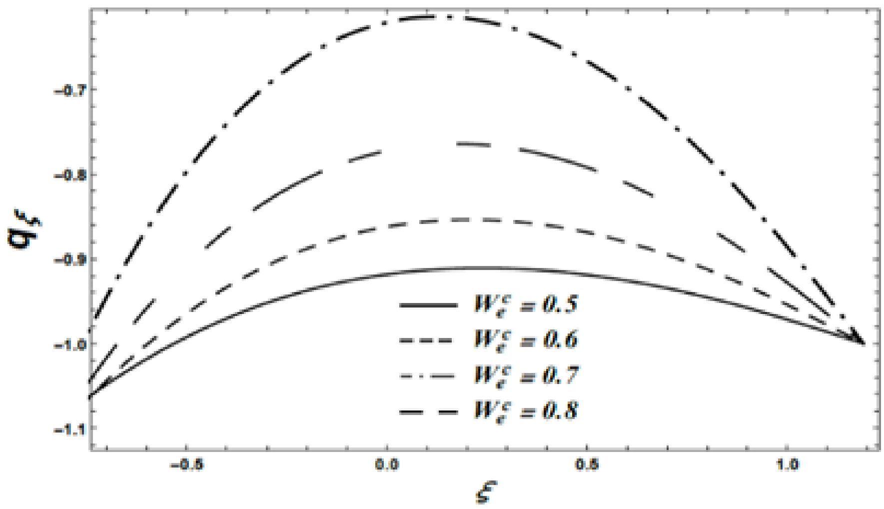


**Fig. 2.** The attitude of $W_e^c$ on $q_\zeta$

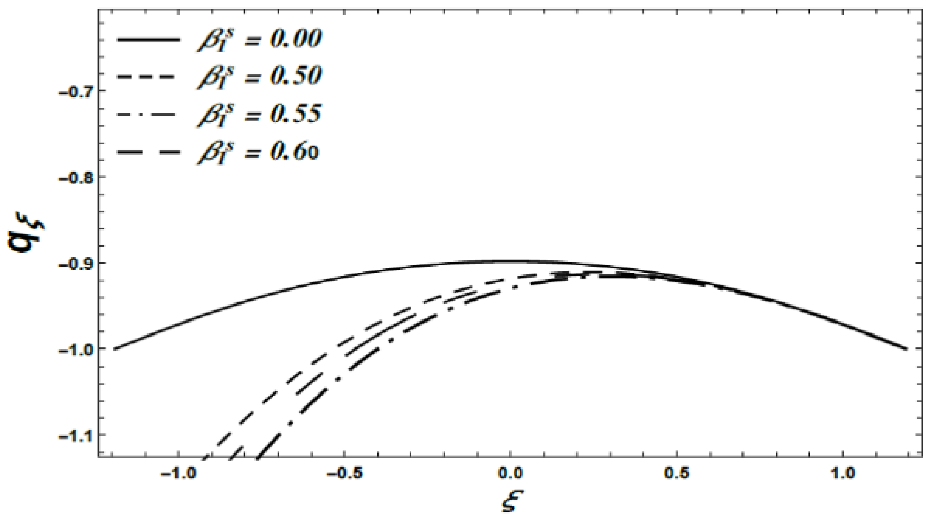


**Fig. 3.** The attitude of $\beta_1^s$ on $q_\zeta$

Figure 4 displays the impact of $\Gamma_H$ on $\theta_E$. As seen from this figure, the $\theta_E$ dwindles with the rise in $\Gamma_H$. From physical perspective, the enhancement in $\Gamma_H$ causes a non-conducting behavior. Moreover, one found that more time is required for the particles to carry heat to its neighboring one, which reduces $\theta_E$. Furthermore, $\theta_E$ enlarges when $\Gamma_H = 0$. This resultant outcome is compatible with the that illustrated by [8], [9], [10], [11], [13], [30], and [39]. The influence of $\gamma_c$ on $\theta_E$ is exhibits through Figure 5. It is found that $\theta_E$ is enriched with the elevation in $\gamma_c$. In fact, when an extra force is added to the fluid which obstruct the flow of the fluid, this resistance causes a couple force, therefore a couple stress is induced in the fluid. This type of fluid is known as couple stress fluid. This obtained result is in good agreement with that represented by [30].

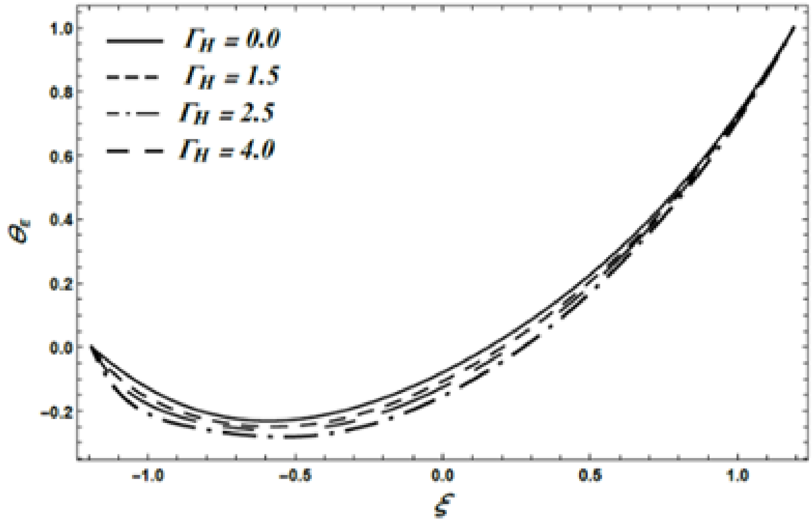


**Fig. 4.** The influence of $\Gamma_H$

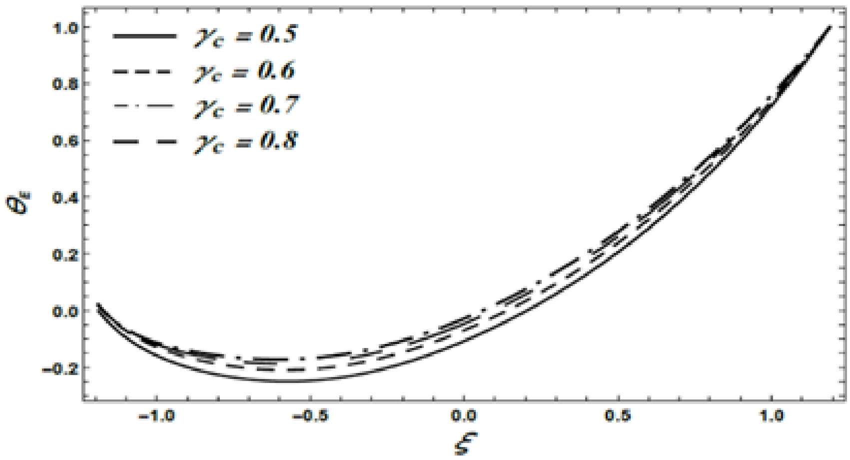


**Fig. 5.** The influence $\gamma_c$ on $\theta_E$

The impacts of $M_F$, $N_{br}$, $D_f$and $S_{or}$ on $\theta_E$ are also studied. It's realized that $\theta_E$ is enhanced with an enhancement in$M_F$. This resultant outcome is compatible to [48]. The impact of $N_{br}$ on $\theta_E$ is illustrated. one found that an enhancement in $N_{br}$ enlarges $\theta_E$. This resultant outcome is compatible with that illustrated by [9], [15] and [33]. Finally, $\theta_E$ has a progressive reduction for diverse values of both $D_f$ as well as $S_{or}$. It is revealed that $\theta_E$ elevates for the growth in $D_f$ together with $S_{or}$ . In fact, the enrichment in both $D_f$ as well as $S_{or}$elevates the thermal-diffusion, and consequently the temperature $\theta_E$ rises. From the physical situation, the diffusion-thermo is known as a heat influx conducted when a chemical system undergoes a concentration gradient. These influences are essentially relied on thermal-diffusion. Mass diffusion is pursued by the disparate distribution of species producing a concentration gradient. Furthermore, a temperature gradient may be considered as a driving force for mass diffusion which is named thermo-diffusion or Soret impact. Thus, the enhancement in the Soret number elevates the temperature gradient. This resultant behavior is totally consistent with that observed by [47]. To avert repetition, these Figures are excluded.

The impact of the Soret number $S_{or}$ on the nanofluid concentration $F_N$ is displayed from Figure 6. It is found, the rising in the Soret number $S_{or}$ enhancing the nanofluid concentration $F_N$. Figure 7 describe the impact of the Schmidt number$S_{ch}$on the nanofluid concentration $F_N$. It is found that $F_N$

dwindles with the elevation in the value of $S_{ch}$. Indeed, $S_{ch}$represents the ratio of thermal diffusivity to mass diffusivity. This is utilized to characterize flows in which there is a simultaneous heat and mass (by convection) transfer. Thus, the enlargement in $S_{ch}$ causes a reduction in the mass diffusion which enriches the inter – molecular force and reduces nanoparticles concentration $F_N$. Also, Schmidt number is inversely proportional to mass diffusivity, that is, the higher the Schmidt number, the less mass diffusivity, hence nano concentration distribution drops. This observed finding corresponds to those observed in [9], [11], [12], [13], [14], [34], [35], and [39].

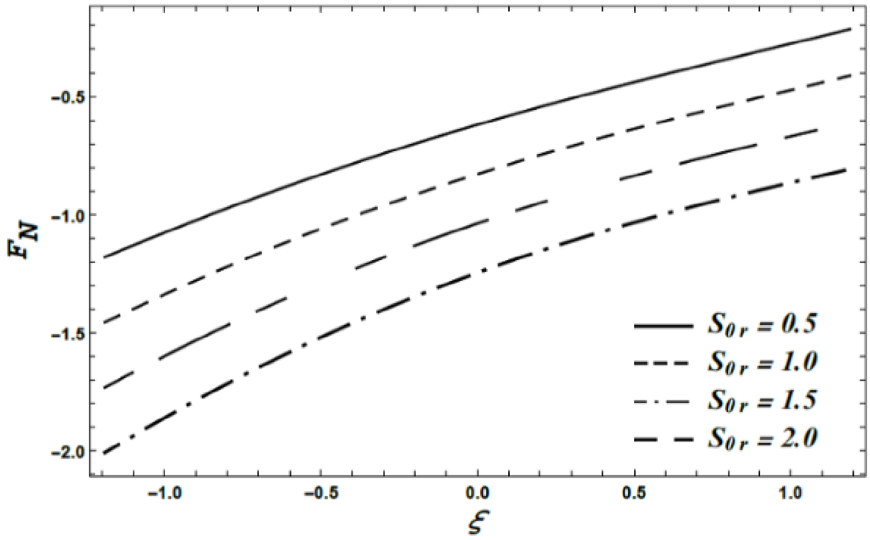


**Fig. 6.** The demeanor of $S_{or}$ on $F_N$

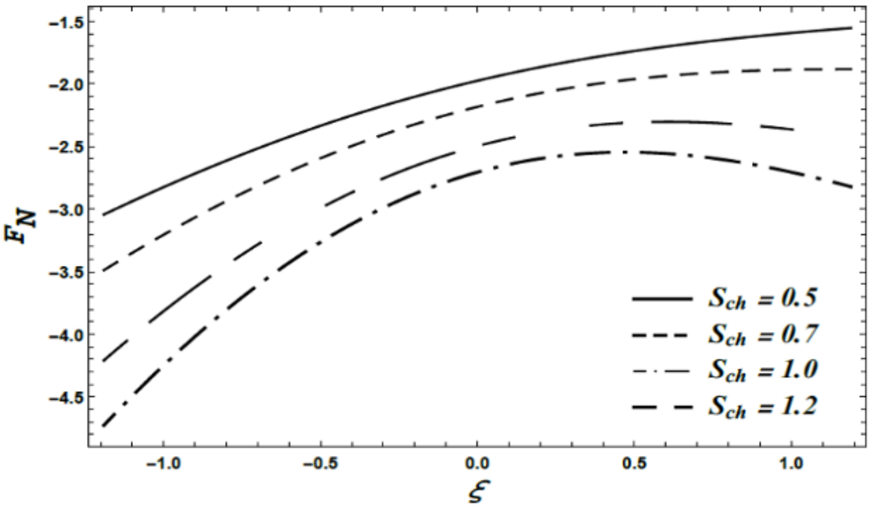


**Fig. 7.** The conduct of $S_{ch}$ on $F_N$

The impacts of $R_{cr}$ and $B_{m1}$ on $F_N$ are examined. It is observed that the conducts of both $R_{cr}$and $B_{m1}$ are as the same as the behavior of $S_{ch}$. The impact of the chemical reaction parameter $R_{cr}$ on the nanofluid concentration $F_N$ is displayed in Figure 6. The enhancing in the chemical reaction parameter $R_{cr}$ is responsible for elevation in the nanofluid concentration $F_N$. In fact, $R_{cr}$ boosts the interfacial mass transfer rate which decays $F_N$. The impact of nano Biot number $B_{m1}$ on the nanofluid concentration $F_N$ is investigated. It is recognized that the rise in $B_{m1}$ causes a progressive reduction in $F_N$. In the physical situation, this behavior takes place since the rise in $B_{m1}$ reduces the thermal conductivity of fluid influx. Thus, the fluid temperature $\theta_E$ is diminished, consequently the nanofluid concentration $F_N$ is decayed. In other words, mass conductivity is dwindled by enlarging in $B_{m1}$, which responsible for decaying in the nanofluid concentration $F_N$. This noticed result is in great agreement with that explained in [35].

## 6. Conclusion

This analytical study target is to exhibits the impact of Cattaneo-Christov heat influx on the peristaltic influx for Carreau nanofluid between two horizontal symmetric channels. The impacts of couple stress, couple stress viscous dissipation, Soret, Dufour, porous medium, heat absorption and chemical reaction are also examined. The governing resulting equations of motion are represented in a dimensionless form. The obtained non-linear system is very complicated to solve analytically. Thus, to relax the complexity of the mathematical procedure, assumptions of long wavelength, together with low Reynolds's number are utilized, followed by the regular perturbation as well as the HPM up to first order. A group of graphs is drawn to describe the influences of the several diverse dimensionless parameters on $q_\zeta$, $\theta_E$ and $F_N$ distributions. The numerical results are found to be in a great agreement with other preceding studies. The concluding remarks may be summarized and outlined as follows

i. $q_\zeta$ is reduced for enlarging in $\beta_1^s, \gamma_c, M_F, D_{Ar}$, whilst it rises with the growth in $W_e^c$.
ii. $\theta_E$ is enhanced for the rise of $M_F$ and $N_{br}$, Meanwhile, $\theta_E$ is reduced for growth in $\Gamma_H$, $D_f, S_{or}$.
iii. $F_N$ is reduced for the rise in $B_{m1}, S_{or}, S_{ch}, R_{cr}$.

## References

[1] Rebhi, Redha, Younes Menni, Giulio Lorenzini, and Hijaz Ahmad. "Forced-Convection Heat Transfer in Solar Collectors and Heat Exchangers: A Review." *Journal of Advanced Research in Applied Sciences and Engineering Technology* 26, no. 3 (2022): 1-15. https://doi.org/10.37934/araset.26.3.115
[2] Salahuddin, T., Mair Khan, and Yu-Ming Chu. "Zero velocity regions near forward and rare points of circular cylinder: A heat and mass transfer study." *Ain Shams Engineering Journal* 12, no. 2 (2021): 2255-2261. https://doi.org/10.1016/j.asej.2020.12.011
[3] Chu, Yu-Ming, Mubbashar Nazeer, M. Ijaz Khan, Farooq Hussain, Huma Rafi, Sumaira Qayyum, and Zahra Abdelmalek. "Combined impacts of heat source/sink, radiative heat flux, temperature dependent thermal conductivity on forced convective Rabinowitsch fluid." *International Communications in Heat and Mass Transfer* 120 (2021): 105011. https://doi.org/10.1016/j.icheatmasstransfer.2020.105011
[4] Shah, Faisal, Muhammad Ijaz Khan, Yu-Ming Chu, and Seifedine Kadry. "Heat transfer analysis on MHD flow over a stretchable Riga wall considering Entropy generation rate: a numerical study." *Numerical Methods for Partial Differential Equations* (2020).
[5] Fourier, Jean Baptiste Joseph, and Gaston Darboux. *Théorie analytique de la chaleur*. Vol. 504. Paris: Didot, 1822.
[6] Cattaneo, Carlo. "Sulla conduzione del calore." *Atti Sem. Mat. Fis. Univ. Modena* 3 (1948): 83-101.
[7] Christov, C. I. "On frame indifferent formulation of the Maxwell–Cattaneo model of finite-speed heat conduction." *Mechanics Research Communications* 36, no. 4 (2009): 481-486. https://doi.org/10.1016/j.mechrescom.2008.11.003
[8] Shah, Faisal, M. Ijaz Khan, Tasawar Hayat, Shaher Momani, and M. Imran Khan. "Cattaneo-Christov heat flux (CC model) in mixed convective stagnation point flow towards a Riga plate." *Computer Methods and Programs in Biomedicine* 196 (2020): 105564. https://doi.org/10.1016/j.cmpb.2020.105564
[9] Masood, Sadaf, Muhammad Farooq, and Shakeel Ahmad. "Description of viscous dissipation in magnetohydrodynamic flow of nanofluid: applications of biomedical treatment." *Advances in Mechanical Engineering* 12, no. 6 (2020): 1687814020926359. https://doi.org/10.1177/1687814020926359
[10] Hayat, Tasawar, Sohail A. Khan, M. Ijaz Khan, Shaher Momani, and Ahmed Alsaedi. "Cattaneo-Christov (CC) heat flux model for nanomaterial stagnation point flow of Oldroyd-B fluid." *Computer Methods and Programs in Biomedicine* 187 (2020): 105247. https://doi.org/10.1016/j.cmpb.2019.105247

[11] Tanveer, A., S. Hina, T. Hayat, M. Mustafa, and B. Ahmad. "Effects of the Cattaneo–Christov heat flux model on peristalsis." *Engineering applications of computational fluid mechanics* 10, no. 1 (2016): 373-383. https://doi.org/10.1080/19942060.2016.1174889

[12] Raja, Muhammad Asif Zahoor, Zeeshan Khan, Samina Zuhra, Naveed Ishtiaq Chaudhary, Wasim Ullah Khan, Yigang He, Saeed Islam, and Muhammad Shoaib. "Cattaneo-christov heat flux model of 3D hall current involving biconvection nanofluidic flow with Darcy-Forchheimer law effect: Backpropagation neural networks approach." *Case Studies in Thermal Engineering* 26 (2021): 101168. https://doi.org/10.1016/j.csite.2021.101168

[13] Kalyani, K., and Sudha Rani MVVNL. "A Numerical Study on Cross Diffusion Cattaneo-Christov Impacts of MHD Micropolar Fluid Across a Paraboloid." *Iraqi Journal of Science* (2021): 1238-1264. https://doi.org/10.24996/ijs.2021.62.4.20

[14] Islam, Saeed, Abdullah Dawar, Zahir Shah, and Adnan Tariq. "Cattaneo–Christov theory for a time-dependent magnetohydrodynamic Maxwell fluid flow through a stretching cylinder." *Advances in Mechanical Engineering* 13, no. 7 (2021): 16878140211030152. https://doi.org/10.1177/16878140211030152

[15] Bashir, Seemab, Muhammad Ramzan, Jae Dong Chung, Yu-Ming Chu, and Seifedine Kadry. "Analyzing the impact of induced magnetic flux and Fourier's and Fick's theories on the Carreau-Yasuda nanofluid flow." *Scientific Reports* 11, no. 1 (2021): 1-18. https://doi.org/10.1038/s41598-021-87831-6

[16] Nazir, Umar, Muhammad Sohail, Umair Ali, El-Sayed M. Sherif, Choonkil Park, Jung Rye Lee, Mahmoud M. Selim, and Phatiphat Thounthong. "Applications of Cattaneo–Christov fluxes on modelling the boundary value problem of Prandtl fluid comprising variable properties." *Scientific Reports* 11, no. 1 (2021): 1-13. https://doi.org/10.1038/s41598-021-97420-2

[17] Ramzan, Muhammad, Hina Gul, Seifedine Kadry, and Yu-Ming Chu. "Role of bioconvection in a three dimensional tangent hyperbolic partially ionized magnetized nanofluid flow with Cattaneo-Christov heat flux and activation energy." *International Communications in Heat and Mass Transfer* 120 (2021): 104994. https://doi.org/10.1016/j.icheatmasstransfer.2020.104994

[18] Gul, Hina, Muhammad Ramzan, Jae Dong Chung, Yu-Ming Chu, and Seifedine Kadry. "Multiple slips impact in the MHD hybrid nanofluid flow with Cattaneo–Christov heat flux and autocatalytic chemical reaction." *Scientific Reports* 11, no. 1 (2021): 1-14. https://doi.org/10.1038/s41598-021-94187-4

[19] Madhukesh, J. K., R. Naveen Kumar, RJ Punith Gowda, B. C. Prasannakumara, G. K. Ramesh, M. Ijaz Khan, Sami Ullah Khan, and Yu-Ming Chu. "Numerical simulation of AA7072-AA7075/water-based hybrid nanofluid flow over a curved stretching sheet with Newtonian heating: A non-Fourier heat flux model approach." *Journal of Molecular Liquids* 335 (2021): 116103. https://doi.org/10.1016/j.molliq.2021.116103

[20] Akaje, Wasiu, and B. I. Olajuwon. "Impacts of Nonlinear thermal radiation on a stagnation point of an aligned MHD Casson nanofluid flow with Thompson and Troian slip boundary condition." *Journal of Advanced Research in Experimental Fluid Mechanics and Heat Transfer* 6, no. 1 (2021): 1-15.

[21] Teh, Yuan Ying, and Adnan Ashgar. "Three dimensional MHD hybrid nanofluid Flow with rotating stretching/shrinking sheet and Joule heating." *CFD Letters* 13, no. 8 (2021): 1-19. https://doi.org/10.37934/cfdl.13.8.119

[22] Rusdi, Nadia Diana Mohd, Siti Suzilliana Putri Mohamed Isa, Norihan Md Arifin, and Norfifah Bachok. "Thermal Radiation in Nanofluid Penetrable Flow Bounded with Partial Slip Condition." *CFD Letters* 13, no. 8 (2021): 32-44. https://doi.org/10.37934/cfdl.13.8.3244

[23] Ismail, Fatiha, Nur Eliyanti Ali Othman, Noorshamsiana Abdul Wahab, and Astimar Abdul Aziz. "The Effect of Chemical and High Pressure Homogenization Treatment Conditions on the Morphology of Nanocellulose." *Journal of Advanced Research in Applied Mechanics* 93, no. 1 (2022): 1-7.

[24] Mahat, Rahimah, Muhammad Saqib, Imran Ulah, Sharidan Shafie, and Sharena Mohamad Isa. "MHD Mixed Convection of Viscoelastic Nanofluid Flow due to Constant Heat Flux." *Journal of Advanced Research in Numerical Heat Transfer* 9, no. 1 (2022): 19-25.

[25] Sharafatmandjoor, Shervin. "Effect of Imposition of viscous and thermal forces on Dynamical Features of Swimming of a Microorganism in nanofluids." *Journal of Advanced Research in Micro and Nano Engineering* 8, no. 1 (2022): 1-8.

[26] Zhao, Tiehong, M. R. Khan, Yuming Chu, A. Issakhov, R. Ali, and S. Khan. "Entropy generation approach with heat and mass transfer in magnetohydrodynamic stagnation point flow of a tangent hyperbolic nanofluid." *Applied Mathematics and Mechanics* 42, no. 8 (2021): 1205-1218. https://doi.org/10.1007/s10483-021-2759-5

[27] Abdal, Sohaib, Imran Siddique, Saima Afzal, Yu-Ming Chu, Ali Ahmadian, and Soheil Salahshour. "On development of heat transportation through bioconvection of Maxwell nanofluid flow due to an extendable sheet with radiative heat flux and prescribed surface temperature and prescribed heat flux conditions." *Mathematical Methods in the Applied Sciences* (2021). https://doi.org/10.1002/mma.7722

[28] Eswaramoorthi, S., Nazek Alessa, M. Sangeethavaanee, Safak Kayikci, and Ngawang Namgyel. "Mixed Convection and Thermally Radiative Flow of MHD Williamson Nanofluid with Arrhenius Activation Energy and Cattaneo–Christov Heat-Mass Flux." *Journal of Mathematics* (2021): 1-16. https://doi.org/10.1155/2021/2490524

[29] Saeed Khan, Noor, Qayyum Shah, and Arif Sohail. "Dynamics with Cattaneo–Christov heat and mass flux theory of bioconvection Oldroyd-B nanofluid." *Advances in Mechanical Engineering* 12, no. 8 (2020): 1-20. https://doi.org/10.1177/1687814020930464

[30] Ibrahim, Wubshet, and Gosa Gadisa. "Double stratified mixed convective flow of couple stress nanofluid past inclined stretching cylinder using Cattaneo-Christov heat and mass flux model." *Advances in Mathematical Physics* (2020): 1-16. https://doi.org/10.1155/2020/4890152

[31] Nagendra, N., B. Venkateswarlu, Z. Boulahia, C. H. Amanulla, and G. K. Ramesh. "Magneto Casson-Carreau Fluid Flow through a Circular Porous Cylinder with Partial Slip." *Journal of Applied and Computational Mechanics* 8, no. 4 (2022): 1208-1221.

[32] Akram, Safia, Maria Athar, Khalid Saeed, Taseer Muhammad, and Mir Yasir Umair. "Partial Slip Impact on Double Diffusive Convection Flow of Magneto-Carreau Nanofluid through Inclined Peristaltic Asymmetric Channel." *Mathematical Problems in Engineering* 2021 (2021). https://doi.org/10.1155/2021/2475846

[33] El-Dabe, Nabil, Galal M. Moatimid, Mona AA Mohamed, and Yasmeen M. Mohamed. "A couple stress of peristaltic motion of Sutterby micropolar nanofluid inside a symmetric channel with a strong magnetic field and Hall currents effect." *Archive of Applied Mechanics* 91, no. 9 (2021): 3987-4010. https://doi.org/10.1007/s00419-021-01990-6

[34] El-Dabe, Nabil, Galal M. Moatimid, Mona AA Mohamed, and Yasmeen M. Mohamed. "Effects of Hall currents with heat and mass transfer on the peristaltic transport of a Casson fluid through a porous medium in a vertical circular cylinder." *Thermal Science* 24, no. 2 Part B (2020): 1067-1081. https://doi.org/10.2298/TSCI180222185E

[35] Yasmin, Humaira, Naveed Iqbal, and Anum Tanveer. "Engineering applications of peristaltic fluid flow with hall current, thermal deposition and convective conditions." *Mathematics* 8, no. 10 (2020): 1710. https://doi.org/10.3390/math8101710

[36] Beleri, Joonabi, and Asha S. Kotnurkar. "Peristaltic Transport of Ellis Fluid under the Influence of Viscous Dissipation Through a Non-Uniform Channel by Multi-Step Differential Transformation Method." *Journal of Advanced Research in Numerical Heat Transfer* 9, no. 1 (2022): 1-18.

[37] Javid, Khurram, Muhammad Riaz, Yu-Ming Chu, M. Ijaz Khan, Sami Ullah Khan, and S. Kadry. "Peristaltic activity for electro-kinetic complex driven cilia transportation through a non-uniform channel." *Computer Methods and Programs in Biomedicine* 200 (2021): 105926. https://doi.org/10.1016/j.cmpb.2020.105926

[38] Hayat, T., Z. Nisar, B. Ahmad, and H. Yasmin. "Simultaneous effects of slip and wall properties on MHD peristaltic motion of nanofluid with Joule heating." *Journal of Magnetism and Magnetic Materials* 395 (2015): 48-58. https://doi.org/10.1016/j.jmmm.2015.07.027

[39] Eldabe, Nabil TM, Mohamed Y. Abou-Zeid, M. E. Ouaf, D. R. Mustafa, and Y. M. Mohammed. "Cattaneo–Christov heat flux effect on MHD peristaltic transport of Bingham Al 2 O 3 nanofluid through a non–Darcy porous medium." *International Journal of Applied Electromagnetics and Mechanics* 68 (2022): 59-84. https://doi.org/10.3233/JAE-210057

[40] He, J. H. "Homotopy perturbation technique, computer methods in applied mechanics and engineering." *International J nonlinear mechanics* 35 (2000): 37-43. https://doi.org/10.1016/S0045-7825(99)00018-3

[41] Abou-Zeid, Mohamed. "Effects of thermal-diffusion and viscous dissipation on peristaltic flow of micropolar non-Newtonian nanofluid: application of homotopy perturbation method." *Results in Physics* 6 (2016): 481-495. https://doi.org/10.1016/j.rinp.2016.08.006

[42] Abou-zeid, Mohamed Y., and Mona AA Mohamed. "Homotopy perturbation method for creeping flow of non-Newtonian power-law nanofluid in a nonuniform inclined channel with peristalsis." *Zeitschrift für Naturforschung A* 72, no. 10 (2017): 899-907. https://doi.org/10.1515/zna-2017-0154

[43] Abou-Zeid, M. Y. "Homotopy perturbation method to gliding motion of bacteria on a layer of power-law nanoslime with heat transfer." *Journal of Computational and Theoretical Nanoscience* 12, no. 10 (2015): 3605-3614. https://doi.org/10.1166/jctn.2015.4246

[44] Farooq, Muhammad, Alamgeer Khan, Rashid Nawaz, Saeed Islam, Muhammad Ayaz, and Yu-Ming Chu. "Comparative study of generalized couette flow of couple stress fluid using optimal homotopy asymptotic method and new iterative method." *Scientific Reports* 11, no. 1 (2021): 1-20. https://doi.org/10.1038/s41598-021-82746-8

[45] Abbas, Wael, Nabil TM Eldabe, Rasha A. Abdelkhalek, Nehad A. Zidan, and Samir Y. Marzouk. "Peristaltic Flow with Heat Transfer for Nano-Coupled Stress Fluid through Non-Darcy Porous Medium in the Presence of Magnetic Field." *Coatings* 11, no. 8 (2021): 910. https://doi.org/10.3390/coatings11080910

[46] Ebaid, Abdelhalim, Fahd Al Mutairi, and S. M. Khaled. "Effect of velocity slip boundary condition on the flow and heat transfer of Cu-water and TiO2-water nanofluids in the presence of a magnetic field." *Advances in Mathematical Physics* (2014): 1-9. https://doi.org/10.1155/2014/538950

[47] El-Dabe, Nabil, and Doaa R. Mostapha. "Hall current effects on electro-magneto-dynamic peristaltic flow of an Eyring–Powell fluid with mild stenosis through a uniform and non-uniform annulus." *Indian Journal of Physics* 96, no. 10 (2022): 2841-2853. https://doi.org/10.1007/s12648-021-02185-z

[48] El-dabe, Nabil TM, and Doaa R. Mostapha. "MHD PERISTALTIC FLOW OF A WALTER'SB FLUID WITH MILD STENOSIS THROUGH A POROUS MEDIUM IN AN ENDOSCOPE." *Journal of Porous Media* 22, no. 9 (2019). https://doi.org/10.1615/JPorMedia.2019025922